On Optimal Solutions to Planetesimal Growth Models

Duncan Forgan[1] and Peter Richtárik[2]

[1] *Scottish Universities Physics Alliance (SUPA), Institute for Astronomy, University of Edinburgh, Blackford Hill, Edinburgh, EH9 3HJ, Scotland, UK*
[2] *Edinburgh Research Group in Optimization (ERGO), School of Mathematics, University of Edinburgh, James Clerk Maxwell Building, EH9 3JZ, Scotland, UK*

ABSTRACT

As expressions are developed which describe planetesimal collisions, it is instructive to find probability distributions for planetesimal parameters which maximize growth of the planetesimal system. Finding such optimal distributions provides clues as to the general efficiency of planet formation, and may help astronomers to determine whether young systems are likely to form planets.

We consider one such collision expression (Stewart & Leinhardt 2009) and propose a simple parametric model of a planetesimal system defining its structure and the way in which collisions occur, which allows us to pose the question of finding systems in which collisions lead to maximum expected growth. We show that this leads to what is known in the optimization literature as a "standard quadratic program". In general, the quadratic function to be minimized is non-convex, which makes the problem computationally intractable. We describe several algorithms for solving problems of this type, and present probability distributions for mass with approximately optimal growth factors.

Assuming that the planetesimal velocity distribution is known, we find that there are many probability distributions of mass that are close to optimal. This might lead one to naively assume that planet formation is a relatively optimal process - however, this result ignores the dependence of planetesimal velocity on mass, and further work is required to determine the effects of the coupling of mass and velocity distributions through physical processes such as aerodynamic drag, turbulence and gravitational scattering. However, this work has demonstrated that optimal solutions for planetesimal growth do not depend strongly on the initial mass distribution.

Key words: planets and satellites: formation - methods: analytical

1 INTRODUCTION

The protoplanetary discs are believed to be the favoured sites of planet formation. Initially composed of gas mixed with interstellar dust grains of varying sizes, this material will eventually assemble itself into planets, satellites, comets, asteroids and other orbiting debris observed in our Solar System and in others. Planet formation theories rely crucially on the criteria which govern fragmentation or coagulation of planetesimals undergoing collisions (Safronov 1972; Weidenschilling & Cuzzi 1993). This is true not just for core accretion theory (Pollack 1996), which requires planets to form in a bottom-up process directly from the collision of dust grains, but also for planet formation by gravitational instability, as the grains are expected to undergo potentially enhanced collisional evolution in the spiral structures induced by marginally unstable protostellar discs (Rice et al. 2004; Clarke & Lodato 2009), or inside the collapsing gaseous envelopes of disc fragments (Boley & Durisen 2010; Nayakshin 2011).

Collisionally growing planetesimals[1] encounter several obstacles in their evolution towards objects approaching planetary masses. The first is environmental in origin: aerodynamic drag exerted by the gas on the dust tends to remove angular momentum, causing radial drift onto the central star (Weidenschilling 1977). This drag is most effective upon grains of approximately metre sizes, removing dust from the system on timescales as short as a few hundred years.

The second obstacle to grain growth is fragmentation as an outcome of planetesimal-planetesimal collisions (Jones et al. 1996). The probability of fragmentation typically increases with grain size until the planetesimals are of approximately decimetre size. Once past this bottleneck, the probability of fragmentation begins to decrease with increasing size, and the planetesimals can grow more efficiently. At smaller grain sizes and lower collision

---

[1] In this paper, we define "planetesimals" to be rocky bodies between millimetre and kilometre size.

velocities, the bouncing barrier (Zsom et al. 2010; Windmark et al. 2012) can also prevent further growth.

Stewart & Leinhardt (2009) developed a velocity-dependent model to describe fragmentation, which compares the reduced mass kinetic energy of the system (Q_R) with the catastrophic disruption criterion (Q_{RD}^*), where the latter quantity is fitted to a mixture of numerical and experimental data (see section 2 for more details). By doing this, they identify a universal law for the mass of the largest remnant of two-body collisions, m_{lr}, where the number of bodies remaining after the collision is unknown.

If we are to understand the efficiency with which protostellar disc systems will form planets, it is useful to investigate to what extent planetesimal growth is optimized, and what distributions of mass and velocity are required to produce optimized growth. For an optimization approach to function fully, an accurate description of the combined mass-velocity probability distribution is required, as the gas in the protostellar disc exerts size/mass-dependent forces such as turbulence and aerodynamic drag, encoding a mass dependence to any velocity distribution.

The exact form of this combined distribution is currently unclear (Dullemond & Dominik 2005), but our understanding is improving as numerical modelling progresses (see for example Ormel & Cuzzi 2007; Garaud et al. 2013, and references within). In the meantime, we can progress by *assuming the mass and velocity probability distributions are independent* (and recognising the limitations that assumption brings). This allows us to immediately apply a series of standard optimization techniques. While more limited in physical application, our results shed light on the efficiency of planet formation.

The structure of the paper is as follows: we begin by describing equations which govern two-body planetesimal collisions derived by Stewart & Leinhardt (2009) in section 2. In section 3 we propose a discrete multibody model, which formalizes i) the structure of a planetesimal system based on a number of parameters, notably the masses and velocities of the planetesimals in the system and their distribution, and ii) a probabilistic scheme in which collisions occur between planetesimals in the system. This allows us to consider the notion of an expected growth factor of a planetesimal system and to search for systems with optimal (i.e., as large as possible) growth factors. Our model has several limiting assumptions; the ramifications of our results are discussed in section 5 and the work is summarized in section 6.

2 TWO-BODY PLANETESIMAL COLLISIONS IN THE STEWART-LEINHARDT PARADIGM

The model of Stewart & Leinhardt (2009) describes the collision of two planetesimals, with masses m_i and $m_{i'}$, and velocities v_j and $v_{j'}$. The reduced mass kinetic energy is:

$$Q_R = \frac{m_{red}v_{rel}^2}{2m_{tot}}, \quad (1)$$

where $m_{red} = \frac{m_i m_{i'}}{m_{tot}}$ is the reduced mass of the projectile and the target, $m_{tot} = m_i + m_{i'}$, and v_{rel} is the relative velocity between the two objects. This is then compared to the catastrophic disruption criterion Q_{RD}^*, which is defined as the value of Q_R such that the mass of the largest remnant m_{lr} is equal to half the total mass. Q_{RD}^* is fitted as a function of a radius equivalent to the total mass contained in a sphere at density $1\,\mathrm{g\,cm^{-3}}$, R_{C1}:
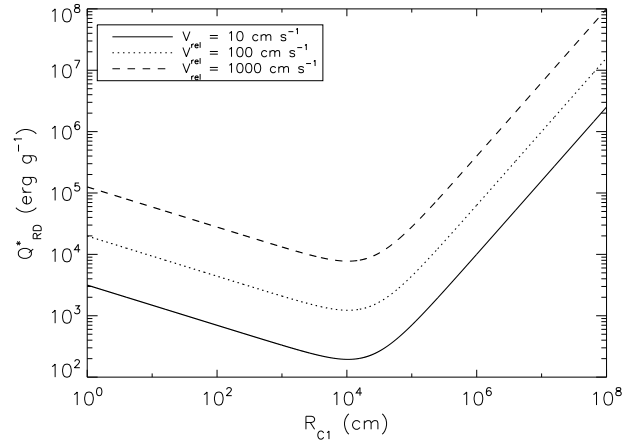
Figure 1. Q_{RD}^* plotted against R_{C1} for several values of the relative velocity V_{rel}. Note the turnover at objects with typical size of tens of metres.

$$R_{C1} = \left(\frac{3m_{tot}}{4\pi}\right)^{\frac{1}{3}}. \quad (2)$$

The expression for Q_{RD}^* is:

$$Q_{RD}^* = q_s R_{C1}^{\frac{9\mu}{3-2\phi}} v_{rel}^{2-3\mu} + q_g R_{C1}^{3\mu} v_{rel}^{2-3\mu}, \quad (3)$$

where μ and ϕ are constants based on material properties, and q_s and q_g are scaling parameters. As with most models of planetesimal collisions, two regimes can be observed in this equation: the "strength" regime, where collisional outcomes are governed by the bodies' tensile strengths, and the "gravity" regime, where the gravitational field is more significant. The fitting of these parameters is based on data derived from numerical simulations of low velocity collisions using PKDGRAV (Richardson 2000; Leinhardt 2000), and previous results for high velocities (Stewart & Leinhardt 2009 and references within). We plot Q_{RD}^* in Figure 1 for several values of relative velocity. Note that for $\mu > 2/3$ (which is typically the case), Q_{RD}^* will always decrease with increasing relative velocity, and hence collisions are more likely to produce fragments with masses less than half the total available mass.

The *growth factor*—the mass of the largest remnant divided by the sum of the masses of the colliding bodies—is given by

$$G \stackrel{\mathrm{def}}{=} \frac{m_{lr}}{m_{tot}} = 1 - \frac{Q_R}{2Q_{RD}^*}. \quad (4)$$

As required by the definition of Q_{RD}^*, it can be seen that when $Q_R = Q_{RD}^*$, we have $G = 1/2$. The total number of fragments remaining after the collision is not quantified. In the strength regime, the largest remnant is a single fragment, whereas in the gravity regime the largest remnant is typically a re-accumulated rubble pile.

This symmetric definition of target and projectile differs somewhat to previous disruption models (i.e., swapping i and i' in this model has no effect on the expression for m_{lr}). The mass of the largest remnant can be expressed as a function of the masses and velocities of the two bodies:

$$m_{lr} = m_{lr}(m_i, m_{i'}, v_j, v_{j'}). \quad (5)$$

By inputting probability distributions for mass and velocity—distributions characterizing the frequency with which a planetesimal of a given mass and velocity appears in a planetesimal system—we can calculate an *expected growth factor of the system*. We are interested in investigating which probability distributions result in the largest expected growth factor.

3 DISCRETE MULTIBODY MODEL (DMM)

In this section we introduce an idealized model describing

(i) the *structure* of a *planetesimal system* (a collection of bodies/planetesimals each of which has mass and velocity belonging to a prescribed discrete set of masses and velocities),

(ii) the way the planetesimals *interact/collide* and

(iii) an objective measure of the *growth potential* of the system: *expected growth factor*.

We consider the problem of finding planetesimal systems with maximum expected growth factor.

3.1 Structure of a Planetesimal System

We say that a planetesimal is of *type* T_{ij} if it has mass m_i and velocity v_j, where $0 < m_1 < m_2 < \cdots < m_I$ and $0 < v_1 < v_2 < \cdots < v_J$. That is, we consider $I \times J$ planetesimal types. The values $\{m_i\}$ and $\{v_j\}$ can be obtained by discretization of intervals of interest; in this section we assume they are given.

Let $\Delta_n \overset{\text{def}}{=} \{d \in \mathbf{R}^n \ : \ \sum d_i = 1, \ d \geqslant 0\}$. That is, Δ_n is the set of n-dimensional vectors with nonnegative entries/coordinates adding up to 1 (probability vectors). Fixing $p \in \Delta_I$ and $q \in \Delta_J$, let $\mathcal{S}(p, q)$ denote a (finite or infinite) system of planetesimals (bodies) such that a $p_i q_j$ proportion of all planetesimals is of type T_{ij} (see Figure 2). Let us pause to explore the consequences of this assumption:

(i) A planetesimal chosen uniformly at random from $\mathcal{S}(p, q)$

    (a) is of type T_{ij} with probability $p_i q_j$,
    (b) has mass m_i with probability $p_i = \sum_j p_i q_j$,
    (c) has velocity v_j with probability $q_j = \sum_i p_i q_j$.

(ii) The distribution of velocities of planetesimals of different masses is the same.

It is clear that (ii) is not physical, due to a variety of different factors. However, it remains a useful simplification for the time being, and remains an issue to be resolved in future work (see later sections).

3.2 Modeling Collisions

We assume that the probability that planetesimals of types $T_{i,j}$ and $T_{i',j'}$ collide (we care about the order) is equal to the probability of randomly selecting two planetesimals of these types from $S(p, q)$ (with replacement); that is, it is given by

$$(p_i q_j)(p_{i'} q_{j'}) = p_i q_j p_{i'} q_{j'}. \tag{6}$$

For finite systems this is equivalent to saying that collisions between any two planetesimals (not types) is equally likely. One can easily verify that the probabilities in (6) add up to unity:

$$\sum_{i,j,i',j'} p_i q_j p_{i'} q_{j'} = (\sum_i p_i)(\sum_j q_j)(\sum_{i'} p_{i'})(\sum_{j'} q_{j'}) = 1. \tag{7}$$

Figure 2. The area of the rectangle corresponding to (m_i, v_j), which is equal to $p_i q_j$, gives the proportion of the planetesimals in the system $\mathcal{S}(p, q)$ of type T_{ij}.

We further assume that when planetesimals of types $T_{i,j}$ and $T_{i',j'}$ collide, the *growth factor* can be written as

$$G(i, j, i', j') = 1 - \tfrac{1}{2} M(i, i') V(j, j'), \tag{8}$$

where, apart from constants, $M(i, i')$ depends on m_i and $m_{i'}$ only, $V(j, j')$ depends on v_j and $v_{j'}$ only, $M(i, i') = M(i', i) \geqslant 0$ and $V(j, j') = V(j', j) \geqslant 0$.

In the rest of the text we will treat M and V as matrices in $\mathbf{R}^{I \times I}$ and $\mathbf{R}^{J \times J}$, respectively. For instance, $M(i, i')$ will be the entry in the i-th row and i'-th column of M.

Define $\nu_{i,i'} = \frac{2}{M(i,i')}$. That is, $\nu = \nu_{i,i'}$ is the maximum value for which $1 - \tfrac{1}{2} M(i, i') \nu$ is nonnegative.

Note that the above assumption is satisfied for the 2-body collision model described in section 2. Indeed, in view of (1), (2) and (3), the growth factor (4) is of the form (8), where

$$M(i, i') = \frac{0.5 m_i m_{i'}}{q_s (\frac{3}{4\pi})^{\frac{3\mu}{3-2\phi}} m_{tot}^{\frac{3\mu}{3-2\phi}+2} + q_g (\frac{3}{4\pi})^{\mu} m_{tot}^{\mu+2}}, \tag{9}$$

$$V(j, j') = |v_j + v_{j'}|^{3\mu}, \tag{10}$$

$\mu = 0.4$, $\phi = 7$, $q_s = 500$ and $q_g = 10^{-4}$. These four constants describe weak aggregates (other constants for strong rocks can be found in Stewart & Leinhardt 2009). We will assume weak aggregate parameters throughout this work.

3.3 Maximizing the Expected Growth Factor

In view of (6) and (8), it is sensible to define the *expected growth factor* of a planetesimal system $\mathcal{S}(p, q)$ as follows:

$$F(p, q) \overset{\text{def}}{=} \sum_{i,j,i',j'} p_i q_j p_{i'} q_{j'} G(i, j, i', j'). \tag{11}$$

Consider now the problem of finding probability vectors p, q *maximizing the expected growth factor*:

$$F^* \overset{\text{def}}{=} \max_{p \in \Delta_I, \ q \in \Delta_J} F(p, q). \tag{12}$$

In other words, we are looking for such distributions of masses and velocities in a planetesimal system for which the average growth

factor is as large as possible. For reasons that will be clear later, we shall also consider the problem of finding the optimal p for *fixed q*:

$$F^*(q) \stackrel{\text{def}}{=} \max_{p \in \Delta_I} F(p, q). \tag{13}$$

Note that

$$F^* = \max_{q \in \Delta_J} F^*(q). \tag{14}$$

In the light of (7), (8) and (11), we can write the expected growth factor in a simpler form:

$$F(p, q) = 1 - \tfrac{1}{2} \left(\sum_{i, i'} p_i p_{i'} M(i, i') \right) \left(\sum_{j, j'} q_j q_{j'} V(j, j') \right)$$
$$= 1 - \tfrac{1}{2} (p^T M p)(q^T V q). \tag{15}$$

Plugging (15) into (12), and noting that the expressions $p^T M p$ and $q^T V q$ must be nonnegative since all entries of the two matrices M, V and vectors p, q are, we obtain the following reformulation of (12):

$$F^* = 1 - \tfrac{1}{2} \left(\min_{q \in \Delta_J} q^T V q \right) \left(\min_{p \in \Delta_I} p^T M p \right). \tag{16}$$

Note that if V is given by (10), then $V(1, 1)$ is the smallest element of V, whence $V(1, 1) \leqslant \min_{q \in \Delta_J} q^T V q$. On the other hand, $q^* = e_1 = (1, 0, 0, \ldots, 0)^T$ attains this lower bound and hence

$$V(1, 1) = \min_{q \in \Delta_J} q^T V q. \tag{17}$$

This means that it is optimal for all planetesimals to have the smallest velocity possible. This is not surprising as the mass of the largest remnant is a decreasing function of the impact velocity. However, it is unrealistic to assume, even though it is theoretically optimal in our model, that all planetesimals in a system will have equal velocity. Even if we did, this velocity would depend on the *choice* of v_1, which is in the hand of the modeler and not in the hands of nature (the modeler constructs the set $\{v_1, \ldots, v_J\}$). We will thus henceforth assume that the distribution of velocities q is *known* (determined via other means than from our model). With this in mind, let us define

$$\theta \stackrel{\text{def}}{=} q^T V q. \tag{18}$$

Note that θ is the impact velocity of an average collision.

It thus seems that problem (13) is a better match for our model than problem (16). The former then reduces to the following optimization problem which is known in the optimization literature under the name *standard quadratic program* or *standard QP*:

$$\min_{p \in \Delta_I} \left[f(p) \stackrel{\text{def}}{=} p^T M p \right]. \tag{19}$$

If p^* is the optimal solution of (19), then in view of (16), the optimal expected growth factor is equal to

$$F^* = 1 - \tfrac{\theta}{2} f(p^*).$$

In section 4 we describe several approaches to solving (19), i.e., to finding the optimal distribution of masses.

Table 1. Summary of the optimization algorithms investigated in this work.

Method	Exact?	Scalable?
Convex Optimization	when f convex	Moderately
2-Coordinate Descent	when f convex	Yes
Nesterov 1/2-solution	1/2-solution	Extremely
Least Squares Convexification	Approximate	Yes

3.4 Individual Growth Factors

It will be useful to define growth factors for each mass m_i, $i = 1, \ldots, I$. That is, we define $F_i(p, q)$ to be the expected growth factor in a random collision with a planetesimal with mass m_i:

$$F_i(p, q) \stackrel{\text{def}}{=} \sum_{i', j, j'} p_{i'} q_j q_{j'} G(i, i', j, j')$$
$$= \sum_{i', j, j'} p_{i'} q_j q_{j'} (1 - \tfrac{1}{2} M(i, i') V(j, j'))$$
$$= 1 - \tfrac{1}{2} \left(\sum_{i'} M(i, i') p_{i'} \right) \left(\sum_{j, j'} q_j q_{j'} V(j, j') \right)$$
$$= 1 - \tfrac{1}{2} (e_i^T M p)(q^T V q)$$
$$\stackrel{(18)}{=} 1 - \tfrac{\theta}{2} e_i^T M p, \tag{20}$$

where $e_i \in \mathbf{R}^I$ is the i-th coordinate vector. Note that by comparing (11) and (20), using the fact that $p = \sum_i p_i e_i$, we see that

$$F(p, q) = \sum_{i=1}^I p_i F_i(p, q). \tag{21}$$

That is, the expected growth factor of a system is equal to an average (expectation) of the individual expected growth factors.

4 OPTIMIZATION METHODS AND RESULTS

In this section we describe several approaches to solving the standard QP problem (19). We illustrate these approaches with examples and computational insights. Table 1 summarizes the optimization techniques we have employed in this work.

4.1 Convex Optimization

If M is positive semidefinite (i.e., if $x^T M x \geqslant 0$ for all x), then f is convex, and problem (19) is solvable using efficient convex optimization algorithms such as interior-point methods (Nesterov & Nemirovski (1994)) or gradient methods (Nesterov (2004)).

Example 1. *For illustration, consider a system with $I = 10$ planetesimals, each with mass $m_i = 10i$, $i = 1, 2, \ldots, 10$. It turns out that M is positive definite and hence f is convex. Using the CVX convex optimization package for MATLAB, we find this system's optimal distribution is $p_1 = 0.5959$, $p_{10} = 0.4041$, and $p_i = 0$ for $i \in \{2, \ldots, 9\}$. This solution is pairing up low mass and high mass planetesimals, and "missing" the more destructive moderate mass region. By slightly favouring the low mass bin, the distribution reduces the probability of massive particles colliding without completely removing them from the system.*

The above example is an exception rather than a rule however;
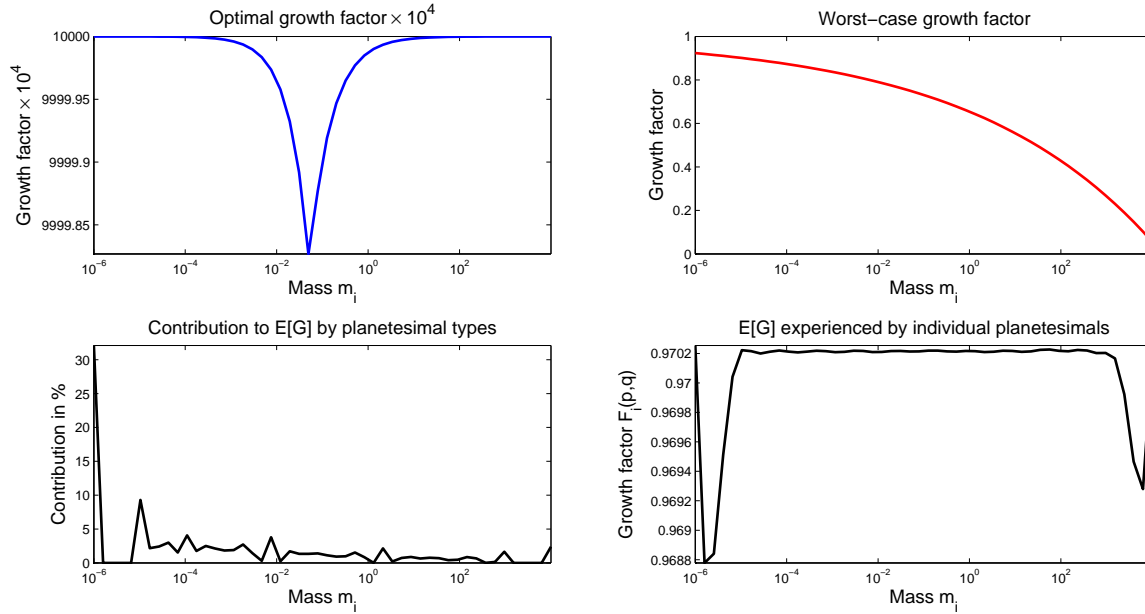
Figure 3. Top Left: Optimal growth factor for each mass is close to 1. That is, for each planetesimal in the system there is another one such that if they collide, the growth factor will be at least 0.99998. **Top Right:** Worst-case growth factor decreases (gets worse) with increasing mass. That is, in the worst case, growth factor of large planetesimals may be small. **Bottom left:** Best p found. We plot the contribution of each planetesimal mass in the system to the overall expected growth factor. What is being plotted for each mass m_i is $p_i F_i(p, q)$ (see Equation (21)). **Bottom right:** Expected growth factors for *individual* planetesimals of mass m_i for best p found, i.e., a p yielding the maximum (total) expected growth factor $\approx 97\%$. For mass m_i we plot $F_i(p, q)$. We have used $\theta = 3,200$.

this is because M will generally not be positive definite. In such a case, convex optimization algorithms are not applicable and we must try other algorithms. From now on we will hence disregard convex optimization as an approach to solving (19).

It turns out that even when f is not convex, a standard QP can be solved exactly provided that I is small (e.g., $I \leqslant 100$) – we refer the reader to Bomze & de Klerk (2001) for further details. However, known approaches do not work well when I is large, and this is the regime we are interested in here. We will hence need to settle for *suboptimal methods* - methods which are not guaranteed theoretically to find the optimal solution - which are able to work in the high dimensional mode.

4.2 A Least-Squares Convexification Approach

As we depict in the bottom right panel of Figure 3, optimal solutions p^* often appear to show *individual* bodies at all masses experiencing similar growth rate, i.e., $F_i(p^*, q)$ does not change with i.

In view of (20), this empirical observation leads to the following algorithmic idea: let us *explicitly search* for probability vector p for which Mp is as close to a vector consisting of identical entries as possible. Letting $e \in \mathbf{R}^I$ be the vector of all ones, $\bar{p} \in \mathbf{R}^I$, and $\|x\| \stackrel{\text{def}}{=} (\sum_i x_i^2)^{1/2}$, this can be achieved by solving the least-squares problem

$$\min_{\bar{p} \geqslant 0} \left[g(p) \stackrel{\text{def}}{=} \|M\bar{p} - e\|^2 \right] \tag{22}$$

and then setting $p = \bar{p}/(e^T \bar{p})$ so as to normalize the output for it to form a probability vector.

Note that g is quadratic and *convex*. Hence, we have replaced the nonconvex (and hence hard) QP (19) by the convex (and hence tractable) QP (22).

Let us now give a theoretical justification for the above approach, which, so far, has been motivated by an empirical observation only. *Assume* that if (19) is solved *without* requiring that $p \geqslant 0$, the solution p^* will, in fact, satisfy $p^* \geqslant 0$ anyway. In that case, the Karush-Kuhn-Tucker optimality conditions (see, e.g., Nocedal & Wright (1999)) imply that

$$\nabla g(p^*) = \lambda e \tag{23}$$

for some constant λ. However, a simple computation shows that $\nabla g(p^*) = 2Mp^*$, whence $2Mp^* = \lambda e$, which is what we wanted to show.

In summary, if the constraint $p \geqslant 0$ "need not be enforced", it is the that $F_i(p^*, q) = const$ for all i.

4.3 A Cyclic 2-Coordinate Descent Method

Here we propose a simple algorithm for approximately solving (19) based on the following idea: given an approximate solution $p \in \Delta_I$, one can try to improve it by picking two distinct planetesimals $i, j \in \{1, \ldots, I\}$ (i.e., two distinct coordinates of the vector p) and reallocating their total weight $p_i + p_j$ among them in an optimal way. That is, we replace p_i by $p_i^+ \geqslant 0$ and p_j by $p_j^+ \geqslant 0$ such that $p_i^+ + p_j^+ = p_i + p_j$, so as to minimize $(p^+)^T Mp^+$, keeping all the other weights constant: $p_l^+ = p_l$ for l other than i and j. It turns out that there is a closed-form solution for p_i^+ and p_j^+. Hence, we propose the following iterative algorithm:

(i) Cycle through all pairs i, j and reallocate weights.

(ii) If, in the last cycle, no reallocation leads to a "sufficient" decrease in the function value, stop. Otherwise, proceed to (i).

Variants of the algorithm we propose above have appeared in the literature under various names. For instance, in machine learning, a similar method is known under the name *sequential minimal optimization* (Platt (1998)), in optimization it is known as *block coordinate descent* (Nesterov (2012), Richtárik & Takáč (2012b), Richtárik & Takáč (2012a), Richtárik & Takáč (2012c)) or *2-coordinate descent* (Necoara et al. (2012), Beck (2012)).

In these variations the choice of the pair (i, j) may be random as opposed to cyclic (randomized methods), or more than 2 coordinates are allowed to be changed at a time (block methods), or the reallocation is allowed to be sub-optimal.

4.3.1 Exponential Discretization

In all experiments in section 5 we let the masses $\{m_i, \ i = 1, 2, \ldots, I\}$ form a uniform discretization, in log scale, of the interval $[\underline{m}, \overline{m}] = [10^{-6}, 10^4]$. That is, we choose

$$m_i = \alpha^{i-1} \underline{m}, \quad i = 1, \ldots, I, \tag{24}$$

where $\alpha = (\overline{m}/\underline{m})^{1/(I-1)}$. Note that $i - 1 = (\log m_i - \log m_1)/\log \alpha$.

Example 2. *If $I = 4$, then matrix M defined in (9) is given by $M = 10^{-3} \times \bar{M}$, where*

$$\bar{M} = \begin{bmatrix} 0.05109400875 & 0.00020300759 & 0.00000021786 & 0.00000000023 \\ 0.00020300759 & 0.11803378641 & 0.00046897376 & 0.00000050330 \\ 0.00000021786 & 0.00046897376 & 0.27267327547 & 0.00108337909 \\ 0.00000000023 & 0.00000050330 & 0.00108337909 & 0.62990141905 \end{bmatrix}.$$

In general, M is nonnegative, symmetric and satisfies the following properties: a) $M(i, i) \leqslant M(i + 1, i + 1)$ for all i, b) $M(i, j - 1) \leqslant M(i, j)$ for all $2 \leqslant j \leqslant i$ and c) $M(i, j) \geqslant M(i, j + 1)$ for $i \leqslant j \leqslant I - 1$.

4.3.2 2-Coordinate Descent via Nested Discretizations

It it natural to expect that the numerical problem of solving the standard QP (19), even approximately, will be more difficult if I is large. On the other hand, one would expect that as the discretization of the interval $[\underline{m}, \overline{m}]$ gets finer, the solution stabilizes in some sense. This leads to the following algorithmic idea: we form a sequence of *nested exponential discretizations* of the interval $[\underline{m}, \overline{m}]$, solving the finer-level problem using the 2-coordinate descent method started from the solution of the problem at the coarser level.

More formally, if at level k we have I_k masses $\{\underline{m} = m_1^k, \ldots, m_{I_k}^k = \overline{m}\}$ then at level $k+1$ we consider $2I_k - 1$ masses $\{m_1^{k+1}, \ldots, m_{2I_k-1}^{k+1}\}$. It can be easily seen that for the exponential discretization described above, necessarily the following nesting property holds: $m_{2i-1}^{k+1} = m_i^k$ for $i = 1, \ldots, I_k$. That is, the masses at level k correspond to the odd-numbered ones. Additionally, the "old" matrix M is a submatrix corresponding to the odd numbered rows and columns of the "new" M. Let $p^k \in \mathbf{R}^{I_k}$ be an approximate solution of (19) at discretization level k. Then we can define $p^{k+1} \in \mathbf{R}^{2I_k-1}$ as follows: $p_{2i-1}^{k+1} = p_i^k$ for $i = 1, \ldots, I_k$ and $p_i^{k+1} = 0$ otherwise, and run the 2-coordinate descent method for this finer discretization, using p^{k+1} as the starting point.

In Figure 4 we show the optimal probability vectors p^k for $k = 1, 2, 3$. At level $k = 1$ we use $I_1 = 3$ masses, at level $k = 2$ we use $I - 2 = 2 \cdot 2 - 1 = 5$ masses, and finally at level $k = 3$ we use $I_3 = 2 \cdot 5 - 1 = 9$ masses. Note that as k increases, the
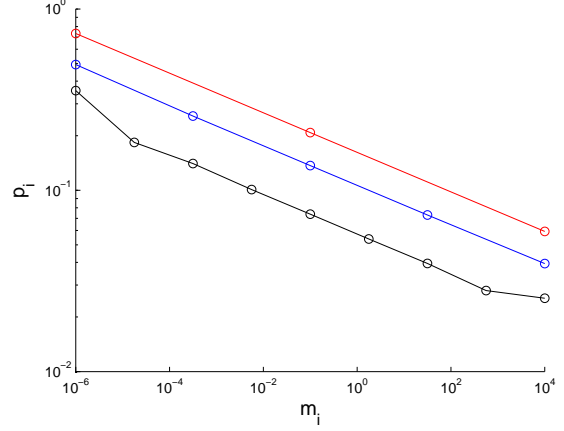
Figure 4. Optimal solutions obtained by the 2-coordinate descent method with nested discretization. Three levels were used: $I_1 = 3$ (red), $I_2 = 5$ (blue) and $I_3 = 9$ (black).
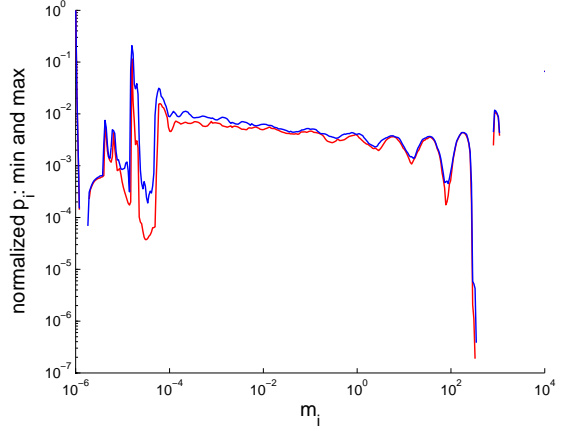
Figure 5. Best solution found for $I = 385$ masses using 2-coordinate descent method with nested discretizaton with 5 levels started with $I_1 = 25$ masses. The method was run 10 times from different random starting probability vectors $p^1 \in \Delta_{25}$. The two lines represent the minimum (red) and maximum (blue) values of p_i (normalized so that $\max_i p_i$ for each of the 10 runs is equal to 1). Note that despite the use of random starting points, the method consistently finds a similar curve. Expected growth factor in all cases $\approx 99\%$ ($\theta = 1,000$).

curve is being shifted downwards. This is to be expected as the sum of all probabilities for each curve is equal to 1, and the number of masses increases. In fact, the curves will converge towards zero as $k \to \infty$. We address the problem of converting p into a true probability distribution function in section 5.3.

In Figure 5 we perform a more serious computation: we compute the near optimal probability vector $p^* = p^5$ using the 2-coordinate descent method with nested discretization, $k = 5$ levels and $I_1 = 25$. The calculation is repeated ten times, each time with an initial starting p selected at random from $\Delta 25$, i.e. the initial p is of length 25, with values randomly selected under the constraint that their sum be unity.

4.4 Nesterov $1/2$-Solutions

Define $f_* = \min_{p \in \Delta_I} f(p)$ and $f^* = \max_{p \in \Delta_I} f(p)$. Fixing $\delta \in [0, 1]$, we say that p is a δ-solution of (19) if

$$f(p) - f_* \leqslant \delta(f^* - f_*). \qquad (25)$$

Let us extend this definition to the maximization problem (12): Vector p is a δ-solution of (12) if

$$F^* - F(p, q) \leqslant \delta(F^* - F_*),$$

where $F_* = \min_p F(p, q)$. Note that if p is a δ-solution of (19), then p is a δ-solution of (12). Indeed,

$$
\begin{aligned}
F^* - F(p, q) \quad &\overset{(16),(15)}{=} \quad (1 - \tfrac{\theta}{2} f_*) - (1 - \tfrac{\theta}{2} f(p)) \\
&= \quad \tfrac{\theta}{2}(f(p) - f_*) \\
&\overset{(25)}{\leqslant} \quad \tfrac{\theta}{2}\delta(f^* - f_*) \\
&= \quad \delta[(1 - \tfrac{\theta}{2} f_*) - (1 - \tfrac{\theta}{2} f^*)] \\
&= \quad \delta(F^* - F_*).
\end{aligned}
$$

Nesterov (1999) proved that there always exists a $\frac{1}{2}$-solution p of (12) of the form $p = (e_i + e_j)/2$ for some $i \neq j$. In other words, for any collection of masses $\{m_1, \ldots, m_I\}$ one can form a simple system consisting of just two such that the expected growth factor of the simple system is "closer" to the optimal growth factor than to the worst-case growth factor:

$$F(p, e_1) \in [\tfrac{1}{2}(F^* - F_*), F^*].$$

Since the growth factor of the worst-case system is nonnegative, this implies that the growth factor of the simple system is not worse than one half of the growth factor of the optimal system.

Physically, Nesterov 1/2-solutions do not possess probability distributions that are likely to be seen in planetesimal systems. They are however interesting mathematically, and can be used as a basis for finding a more physically realistic near-optimal distribution.

5 RESULTS & DISCUSSION

In this section we comment on some computational insights gained from solving the standard QP (19) with $\theta = q^T V q = 3000$ and M as described in Section 3. As our methods can only return a suboptimal p, we run the output from one method as input for another, to refine p, and tend towards larger values of the expected growth factor $F(p, q)$.

5.1 Optimum Growth Factors for Individual Planetesimals

Before attempting to find probability distributions which optimize the total growth factor, it is instructive to investigate individual particle-particle collisions.

The top left panel of Figure 3 shows for each m_i (x-axis) the value

$$\max_j F_i(e_j, q) = \max_j 1 - \tfrac{\theta}{2} e_i^T M e_j = 1 - \tfrac{\theta}{2} \min_j M_{ij}.$$

That is, for each mass m_i in the system we find a mass m_j in the system which leads to the best (highest) growth factor. It can be seen that in general, for any m_i there is a counterpart $m_{i'}$ such that a collision results in a growth factor close to unity. This corresponds to high mass particles being able to accrete low mass particles with ease.

The top right panel shows the worst case growth factor. That is, we plot

$$\min_j F_i(e_j, q) = \min_j 1 - \tfrac{\theta}{2} e_i^T M e_j = 1 - \tfrac{\theta}{2} \max_j M_{ij}.$$

In a sense, this particular plot illustrates some of the most basic obstacles to planet formation, where the growth factor dips below 50% once the particle reaches a mass around 10 grams. The dip towards zero corresponds to massive particles colliding and shattering.

In the bottom left and right panels of Figure 3 we consider the best p for this discretisation level, leading to the expected growth factor

$$E[G] = F(p, q) \approx 0.97,$$

i.e., 97%. In the left panel, for each mass m_i we plot the quantity $p_i F_i(p, q)$, which in view of (21) is the *contribution of all planetesimals of mass m_i* to the expected growth factor $F(p, q)$. We observe that *planetesimal types of light masses contribute more to the overall growth factor than planetesimal types of larger masses*. We do not have a good explanation for the spikes - it is conceivable that these are simply a byproduct of the particular numerical scheme used and not an indication of a genuine physical phenomenon.

In the bottom right panel, for each mass m_i we plot the quantity $F_i(p, q)$, which in view of (20) is the expected growth factor resulting from a random collision in the system with *an individual planetesimal* of type i (i.e., of mass m_i). We observe that *in optimal or nearly optimal systems, individual planetesimals of all masses have approximately the same expected growth factor*.

The conclusion based on the bottom left and panels of Figure 3 is that it is the expected growth factors of *individual* planetesimals, rather than planetesimal types, tend to be about equal in optimised systems. This is a common feature of highly optimised distributions, and it motivated us to develop the "least-squares convexification" algorithm which attempts to explicitly find distributions which have this feature.

5.2 Best Exponential Law

Consider probability vectors $p = p(\beta) \in \Delta_I$ of the form $p_i = p_1/\beta^{i-1}$, $i = 1, 2, \ldots, I$, where $\beta \geqslant 1$. Clearly,

$$\frac{p_i}{p_1} = \frac{1}{\beta^{i-1}} \overset{(24)}{=} \beta^{-\frac{\log(m_i/m_1)}{\log \alpha}} = \left(\frac{m_i}{m_1}\right)^{-\frac{\log \beta}{\log \alpha}}. \qquad (26)$$

Note that p_i depends on m_i exponentially; that is, $\log p_i$ depends on $\log m_i$ linearly, with slope $-\log \beta/\log \alpha$.

We run an experiment with $I = 50$ ($\alpha = 1.59986$) and computed β for which $p^T M p$ is minimized (see (19)). We obtained $\beta = 1.06289$ and expected growth factor $F(p, q) = 98.89\%$ (we used $\theta = 1,000$ ms^{-1}). The log-linear slope is $-\log \beta/\log \alpha = -0.127$; see Figure 6. This is a much shallower slower slope than is typically observed in protoplanetary discs, e.g. the canonical size distribution of $a^{-3/5}$ (D'Alessio et al. 2001; Natta & Testi 2004; Williams & Cieza 2011), which we can convert naively assuming constant density spheres to give $x \approx 1.8$. This would suggest that observed grain size distributions are already sub-optimal for planet formation, even ignoring dynamical effects. However, even at steeper slopes, the growth rate remains relatively high, suggesting that the parameter space for protostellar discs that, by our definition, are close to optimal is quite large.
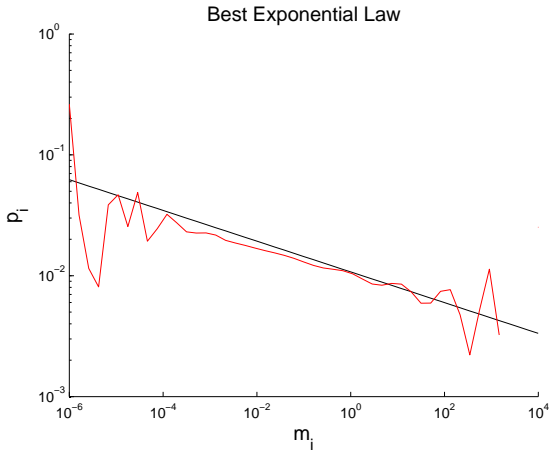
Figure 6. Best exponential law (for $I = 49$) leads to a system with 98.89% expected growth factor and has slope -0.127 (black solid line). The red line corresponds to the vector p obtained by post-processing the best exponential law using our 2-coordinate descent method.

5.3 Estimating the Optimal Continuous Density of Masses

Assume an exponential discretization with step α, as described above. Let c be an arbitrary constant satisfying $1 < c < \max\{\alpha, 2\}$. With each mass m_i, $i = 1, 2, \ldots, I$, we will associate interval $K_i \stackrel{\text{def}}{=} [m_i - A_i, m_i + A_i)$ recursively as follows:

- $A_1 = (c-1)m_1$,
- $A_{i+1} = (\alpha^i - \alpha^{i-1})m_1 - A_i$, $i = 1, 2, \ldots, I - 1$.

Note that $m_i + A_i = m_{i+1} - A_{i+1}$, so that the intervals fully cover $[m_1, m_I]$ and are disjoint. It should be possible to prove that the ratio A_{i+1}/A_i quickly converges to α when we choose $c = (1+\alpha)/2$. That is, the intervals $\{K_i\}$ gets larger at an exponential rate, with factor α, and we approximately have

$$|K_{i+1}|/|K_i| \approx \alpha.$$

Let $p \in \Delta_I$ be an optimal probability vector and define

$$v_i \stackrel{\text{def}}{=} p_i/|K_i| = p_i/(2A_i).$$

The function that maps a mass $m \in K_i$ to v_i should be seen as the "empirical probability distribution function of a continuous version of p". Note that optimal p necessarily depends on the discretization constant α, but that one expects that the vector of densities v will not depend on this. Hence, one would expect that the piecewise-linear curve mapping the masses in $[m_1, m_I]$ to v_i via

$$v_i(\alpha) = p_i(\alpha)/|K_i(\alpha)|$$

"converges" to some stationary curve on $[m_1, m_I]$ as α decreases to 1, i.e., as solutions of finer discretizations are obtained. However, numerically computing v_i (via computing p_i) is challenging for small α as this leads to standard quadratic programs with a huge number of variables.

5.4 Limitations of the Analysis

We have been forced to curtail our analysis with some limiting assumptions, partially through ignorance, and partially through a desire to define a problem that was initially both soluble and comprehensible. We now discuss these limits here.

Above all assumptions made here, the most crucial is the independence of mass and velocity distributions. It is clear from the effects of aerodynamic drag, gravitational scattering, turbulence, and even Poynting-Robertson drag, that the velocity of bodies in planet-forming systems will be a strong function of their mass (Weidenschilling & Cuzzi 1993; Ormel & Cuzzi 2007). The issue is how to describe this influence. The combined effect of a number of physical processes is difficult to characterise by models such as ours. Even simple toy models which describe the processes affecting planetary embryos and planetesimals become rapidly complex (Ormel & Kobayashi 2012; Laibe et al. 2013; Laibe 2013; Laibe et al. 2013).

Future work must attempt to characterise at least some of the dependence of velocity on mass, and relax the assumption of mass and velocity separability. By doing so, the model may also be able to incorporate the effects of impact angle (see e.g. Leinhardt & Stewart 2012), and begin addressing more subtle obstacles to growth such as the bouncing barrier (Zsom et al. 2010; Windmark et al. 2012).

In the calculation of expected growth factors, we have assumed that any two bodies in the system have the same probability of collision. This again is not realistic - the effective cross section of each body will increase with mass. Also, if the spatial distribution of bodies is a function of size the probability of collision must reflect this. This is likely to be the case in most disc systems, which will settle vertically (Goldreich & Ward 1973; Zsom et al. 2011; Laibe et al. 2013). Radial variations in grain size are also common in protostellar and debris disc systems (cf Birnstiel & Andrews 2014 and Müller et al. 2010 respectively). Indeed, the model itself implicitly assumes that there are a large enough number of planetesimals in the system that collisions are equivalent to sampling with replacement, i.e. that equation 6 holds. This approximation will begin to fail in the later stages of planet formation as the number of bodies of a given mass in a given location begins to decrease.

We have also assumed that whenever two bodies collide, it is the mass of the largest remnant that is the most interesting quantity (or at least, the expected value). There are two things to note here:

(i) The mass of the other remnants produced as a result of the collision will play a role in the future growth of the system (Blum 1993; Leinhardt & Stewart 2012), and
(ii) The expected value is only one possible measure of growth potential. Other measures may be more pertinent (such as the number of remnants).

The assumption that two planetesimals with the same mass and velocity are indistinguishable is a related issue. We expect chemical composition (and porosity) of planetesimals to vary, especially with distance from the star. Porosity in particular is demonstrably important in the outcome of planetesimal collisions (Meru et al. 2013).

The snow line (Hayashi 1981; Sasselov & Lecar 2000) is one example of spatial differentiation, but there are many others, including processes such as crystallisation and thermal annealing, or even the formation of chondrites (Boley & Durisen 2008). As a result, using one set of strength regime parameters q_s and ϕ is not realistic - these parameters should be varied between impacts for individual rocks, e.g. collisions that follow strong impacts should use weak aggregate parameters (Stewart & Leinhardt 2009).

The paradigm set out by Stewart & Leinhardt (2009) is not the only means by which planetesimal collision can be modelled. The coagulation equation approach (Dullemond & Dominik 2005) uses integro-differential equations to evolve a discrete population

of planetesimals in gas and dust discs, resolving processes such as rapid radial drift and differential midplane settling. They come across similar uncertainty in describing relative velocities, especially in the case of disc turbulence. Garaud et al. (2013) add stochasticity to these equations, incorporating probability distributions for velocities rather than simply using their mean values.

These models do suggest future avenues of research, where their expressions for relative velocities due to various processes could be incorporated. Probability distributions for velocity at different particle masses (e.g. Ormel & Cuzzi 2007, who develop these relative velocity distributions in turbulence) are non-trivial to generate analytically for all masses, and usually require confirmation through numerical simulations (e.g. Carballido et al. 2010; Hubbard 2012). A simple first step would be to assume the distribution of velocities is Maxwellian, which is indeed the case for sufficiently large particle sizes, and apply optimisation algorithms to this model. At this stage, it is unclear if the shallow slopes for mass probability distributions obtained in this paper will be retained as the relative velocity is more realistically calculated.

6 CONCLUSIONS

We investigate the applicability of optimisation methods to planetesimal growth. Beginning with a prescription for the growth of planetesimals after a two-body collision, we develop a discretised multibody model which calculates the expected growth factor across a planetesimal population defined by probability distributions in mass and velocity.

We assume that the mass and velocity distributions are independent for simplicity. The matrix constructed as a result is typically non-convex, and as a result definitively optimal solutions are not found. We use several algorithms and heuristics to determine near-optimal solutions, and find that many distributions result in close to optimal planetesimal growth.

The typical near-optimal mass distribution approximates a powerlaw, with index less than 1, which is somewhat flatter than expected from canonical grain size distributions observed in debris discs. Larger powerlaw indices are still quite efficient. Mass distributions which are close to optimal display uniform growth of planetesimals at all masses.

This is an oversimplified analysis, especially given the assumption of separable mass and velocity distributions. Even in this simple case, we find that optimisation is non-trivial, and the true optimal distribution cannot be conclusively determined. This is likely to be the case for mass and velocity distributions that are not separated, and we intend to investigate this in future work.

However, what we can demonstrate, even in these simplified circumstances, is that the principal factor in planetesimal growth is not the initial distribution of planetesimal mass, but rather the initial distribution of planetesimal velocities, and how these velocities evolve with time.

REFERENCES

Beck A., 2012, Technical report, The 2-Coordinate Descent Method for Solving Double-Sided Simplex Constrained Minimization Problems

Birnstiel T., Andrews S. M., 2014, The Astrophysical Journal, 780, 153

Blum J., 1993, Icarus, 106, 151

Boley A. C., Durisen R., 2008, ApJ, 685, 1193

Boley A. C., Durisen R. H., 2010, ApJ, 724, 618

Bomze I. M., de Klerk E., 2001, J. Global Optim, 24, 163

Carballido A., Cuzzi J. N., Hogan R. C., 2010, Monthly Notices of the Royal Astronomical Society, 405, no

Clarke C. J., Lodato G., 2009, MNRAS, 398, L6

D'Alessio P., Calvet N., Hartmann L., 2001, ApJ, 553, 321

Dullemond C. P., Dominik C., 2005, A&A, 434, 971

Garaud P., Meru F., Galvagni M., Olczak C., 2013, The Astrophysical Journal, 764, 146

Goldreich P., Ward W. R., 1973, The Astrophysical Journal, 183, 1051

Hayashi C., 1981, Progress of Theoretical Physics Supplement, 70, 35

Hubbard A., 2012, Monthly Notices of the Royal Astronomical Society, 426, 784

Jones A. P., Tielens A. G. G. M., Hollenbach D. J., 1996, ApJ, 469, 740

Laibe G., 2013, Monthly Notices of the Royal Astronomical Society, 437, 3037

Laibe G., Gonzalez J.-F., Maddison S. T., 2013, Monthly Notices of the Royal Astronomical Society, 437, 3025

Laibe G., Gonzalez J.-F., Maddison S. T., Crespe E., 2013, Monthly Notices of the Royal Astronomical Society, 437, 3055

Leinhardt Z., 2000, Icarus, 146, 133

Leinhardt Z. M., Stewart S. T., 2012, The Astrophysical Journal, 745, 79

Meru F., Geretshauser R. J., Schafer C., Speith R., Kley W., 2013, Monthly Notices of the Royal Astronomical Society, 435, 2371

Müller S., Löhne T., Krivov A. V., 2010, ApJ, 708, 1728

Natta A., Testi L., 2004, Star Formation in the Interstellar Medium: In Honor of David Hollenbach, 323, 279

Nayakshin S., 2011, MNRAS, 413, 1462

Necoara I., Nesterov Y., Glineur F., 2012, Technical report, Efficiency of randomized coordinate descent methods on optimization problems with linearly coupled constraints

Nesterov Y., 1999, Technical report, Global Quadratic Optimization on the Sets With Simplex Structure

Nesterov Y., 2004, Introductory Lectures on Convex Optimization. A Basic Course. Vol. 87 of Applied Optimization, Kluwer Academic Publishers, Boston

Nesterov Y., 2012, SIAM J Optimization, pp 341–362

Nesterov Y., Nemirovski A., 1994, Interior-Point Polynomial Algorithms in Convex Programming. Vol. 13 of SIAM Studies in Applied Mathematics

Nocedal J., Wright S. J., 1999, Numerical Optimization. Springer-Verlag

Ormel C. W., Cuzzi J. N., 2007, Astronomy and Astrophysics, 466, 413

Ormel C. W., Kobayashi H., 2012, The Astrophysical Journal, 747, 115

Platt J. C., 1998, Technical report, Sequential Minimal Optimization: A Fast Algorithm for Training Support Vector Machines

Pollack J., 1996, Icarus, 124, 62

Rice W. K. M., Lodato G., Pringle J. E., Armitage P. J., Bonnell I. A., 2004, MNRAS, 355, 543

Richardson D., 2000, Icarus, 143, 45

Richtárik P., Takáč M., 2012a, in Operations Research Proceedings 2011 Efficient serial and parallel coordinate descent method for huge-scale truss topology design. Springer, pp 27–32

Richtárik P., Takáč M., 2012b, Technical report, Iteration complexity of randomized block-coordinate descent methods for minimizing a composite function

Richtárik P., Takáč M., 2012c, Technical report, Parallel coordinate descent methods for big data optimization

Safronov V. S., 1972, Evolution of the protoplanetary cloud and formation of the earth and planets.

Sasselov D. D., Lecar M., 2000, ApJ, 528, 995

Stewart S. T., Leinhardt Z. M., 2009, ApJ, 691, L133

Weidenschilling S. J., 1977, MNRAS, 180, 57

Weidenschilling S. J., Cuzzi J. N., 1993, In: Protostars and planets III (A93-42937 17-90), pp 1031–1060

Williams J. P., Cieza L. A., 2011, eprint arXiv:1103.0556

Windmark F., Birnstiel T., Güttler C., Blum J., Dullemond C. P., Henning T., 2012, A&A, 540, A73

Zsom A., Ormel C. W., Dullemond C. P., Henning T., 2011, Astronomy & Astrophysics, 534, A73

Zsom A., Ormel C. W., Güttler C., Blum J., Dullemond C. P., 2010, Astronomy and Astrophysics, 513, A57